ISPRS Annals of the Photogrammetry, Remote Sensing and Spatial Information Sciences, Volume XI-2-2026
XXV ISPRS Congress 2026 “From Imagery to Understanding”, Commission II, 4–11 July 2026, Toronto, Canada

Image LiDAR based change detection and updating for urban 3D reconstruction

Teng Wu, Bruno Vallet

Univ Gustave Eiffel, Géodata Paris, IGN, LASTIG, F-77454 Marne-la-Vallée, France

Keywords: 3D reconstruction, Change detection, Ray tracing, Image LiDAR fusion, Mesh processing

Abstract

There is a high demand for accurate and up-to-date territorial digital twins for human activities, but their production and updating costs remain prohibitive for many applications. Their generation relies on acquiring LiDAR and/or image data over the territory of interest. Each modality has its advantages: LiDAR is more accurate but more costly, while images are noisier but less costly and more easily accessible. Combining these two technologies to produce and update digital twins is thus a promising avenue. In this paper, we propose a pipeline based on 3D change detection to update a LiDAR point cloud using newer aerial imagery. First, triangle meshes are generated from LiDAR data and image-based dense matching. Then, 3D ray tracing is used to detect changes. After removing the changed parts, the point clouds are fused to update the scene. The proposed method is demonstrated on two datasets in France. The code will be open source on Github: https://github.com/whuwuteng/ChangeUpdateJN.

1. Introduction

3D reconstruction plays a crucial role in the development of digital twins. Among various data sources, images and LiDAR are the most widely used. Traditional 3D reconstruction methods based solely on photogrammetry often fail in regions with low texture, specular surfaces, or complex geometries. In contrast, LiDAR systems provide dense and accurate point clouds but lack continuous radiometric information, and their acquisition cost is relatively high. To achieve a high-accuracy digital twin at a lower cost, one effective strategy is to use a high-quality LiDAR mesh as the reference geometric representation and employ lower-quality image-based dense matching to update it only where the scene has changed, in order to preserve the high quality where the scene remains static. Consequently, change detection becomes a key component of the updating process.

However, change detection is a complex subject because defining the types of changes of interest is challenging, and real-world changes cannot be easily categorized. Numerous studies have addressed this topic, most of which focus on detecting changes between two images captured from the same or nearly the same viewpoint. For geometric change detection, digital surface model (DSM) comparison and point cloud distance-based methods are commonly adopted. Nevertheless, image/LiDAR change detection and updating provide a cost-effective solution for maintaining digital twins.

Currently, many countries are conducting nationwide LiDAR acquisition campaigns, such as the height model of the Netherlands (Actueel Hoogtebestand Nederland, AHN) (Swart, 2010) and LiDARHD in France. The density of AHN is about 6 points/m^2, and the density of LiDARHD is about 10 points/m^2. Since LiDAR acquisition is expensive, new nationwide acquisitions are typically performed only every few years. Meanwhile, aerial and satellite imagery is frequently collected to derive geoinformation products. Therefore, integrating aerial or satellite images with existing LiDAR can significantly improve the timeliness of digital twins. With the widespread use of Unmanned Aerial Vehicles (UAVs) in photogrammetry, it is now possible to obtain temporally up-to-date datasets, albeit with relatively lower geometric accuracy. For updating, UAVs can be used within a framework where significant changes are first detected, and then a UAV is deployed to map these changes. As a result, data updating strategies that consider both temporal and geometric quality have become increasingly important in current applications.

In this paper, we propose a complete pipeline that combines aerial LiDAR and images to produce an updated 3D model, maximizing the quality and timeliness of the input sources Figure 1. The proposed method includes sensor mesh generation, 3D change detection, and point cloud updating. The main contributions of this work are summarized as follows:

- A 3D pipeline for updating LiDAR point clouds using images.
- A quality-aware strategy for point cloud updating.
- A 3D change detection approach based on sensor mesh representation.

The paper is structured as follows: The state of the art is introduced in Section 2. The proposed method is described in Section 3. Experiments and analysis are provided in Section 4. Finally, conclusions are drawn and perspectives are discussed in Section 5.

2. Related Work

This paper focuses on urban point cloud change detection and updating based on 3D models. It consists of two parts: mesh generation (3D reconstruction), and change detection and updating.

2.1 3D Reconstruction

3D reconstruction is a widely explored topic. In photogrammetry, two major approaches are commonly used: image-based and LiDAR-based reconstruction (Wang, 2013). Image-based 3D reconstruction has been extensively studied, covering various aspects such as dense image matching (Remondino et al., 2014), mesh generation (Vu et al., 2011), and texture mapping

This contribution has been peer-reviewed. The double-blind peer-review was conducted on the basis of the full paper.
https://doi.org/10.5194/isprs-annals-XI-2-2026-385-2026

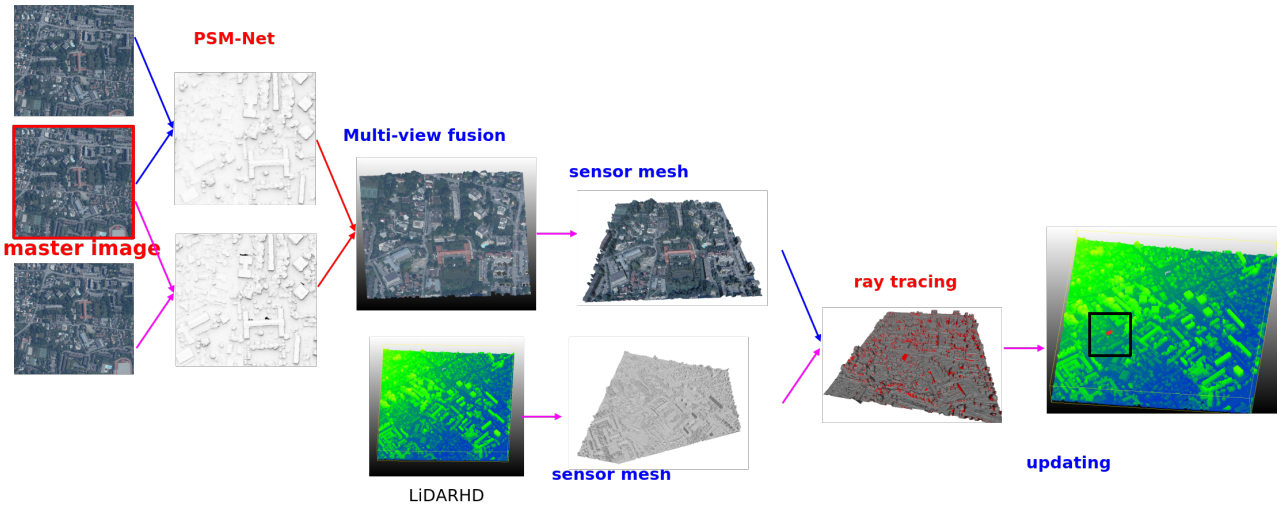

Figure 1. The workflow of the proposed method is as follows. LiDARHD is treated as an old but highly accurate data source, while the aerial images are considered new and are used to update only the changed areas. Deep learning–based stereo dense matching is applied to obtain a point cloud from multi-view images, and sensor meshes are generated from both the image data and the LiDAR data. Ray tracing is then used for change detection. After removing the detected changes, the new point cloud derived from the images is fused into the LiDAR point cloud.

(Waechter et al., 2014). With the advancement of deep learning, stereo dense matching (Laga et al., 2020) and multi-view stereo (MVS) methods (Wang et al., 2021) have been increasingly enhanced or replaced by neural network–based techniques. 3D reconstruction from point clouds has also been widely investigated (Sulzer et al., 2024).

In this work, only mesh generation is considered. Typical approaches include surface reconstruction using Poisson methods (Kazhdan et al., 2006), where estimating accurate normals remains challenging, and graph-cut-based methods (Labatut et al., 2009), which may struggle to define consistent visibility or optical centers, especially in cases with missing data.

2.2 Change Detection and Updating

Change detection has become an increasingly important topic, as urban development progresses slowly and timely updates can significantly improve the temporal quality of digital twins. This problem has been widely studied, particularly in 2D image domains (Wen et al., 2021), with deep learning-based approaches showing remarkable progress (Bai et al., 2023). However, 2D image-based change detection often relies on orthophotos, which are affected by occlusions, especially in urban areas with tall buildings (Pang et al., 2023).

In 3D space, change detection is typically performed using point clouds (Xiao et al., 2023, Stilla and Xu, 2023). For pure LiDAR change detection, ray tracing is usually used (Xiao et al., 2015), but point-based occupancy depends on the point size, which is difficult to estimate; mesh-based approaches can avoid this problem (Wu et al., 2023). Similarity maps can also be used for change detection (Aijazi et al., 2013a). Detecting changes between image-derived and LiDAR-derived data is considerably more difficult due to differences in data modality, density, and noise characteristics. Change detection can be performed using DSM differencing combined with correlation matching (Du et al., 2016); geometrical consistency after projection of point clouds and stereo images has also been used to detect changes (Qin and Gruen, 2014). (Zhou et al., 2020) proposed a method that uses LiDAR data to guide dense image matching and handle scene changes, but the output remains an image-based DSM rather than a fully integrated 3D representation.

For 3D model updating, simple fusion is often applied after removing inconsistent points (Wu et al., 2016). Incremental updating can also be performed using object fusion functions (Aijazi et al., 2013b), and surface cutting can be used to fuse two models (Zhang et al., 2024).

3. 3D base Change detection and update

In this paper, we propose a fully 3D-based change detection pipeline. It consists of several steps: (1) mesh generation from LiDAR, (2) mesh generation from images, and (3) 3D change detection and point cloud updating.

3.1 Mesh generation from LiDAR

Because we aim to preserve the optical center and keep the LiDAR point cloud as much as possible, a sensor mesh (Boussaha et al., 2018) is used. However, a key difference is that aerial LiDAR data are distributed in LAS/LAZ format, where some information (for example, scan order and the start and end of scan lines) is missing in the distributed data. Since the GPS time is preserved, it is used to recover the separated scan lines. The scan lines are then linked using 2D triangulation to produce the mesh, as illustrated in Figure 2. We link successive scans accordingly, and then obtain the sensor mesh, as shown in Figure 3. This method proves to be much faster than traditional point cloud reconstruction methods.

Because the GPS trajectory is also provided, we can estimate the optical center for each echo using GPS time interpolation. The optical center can then be used for ray tracing.

3.2 Mesh generation from images

In this work, we assume that the image mesh (the lower-quality data) is more recent than the LiDAR mesh. To generate the

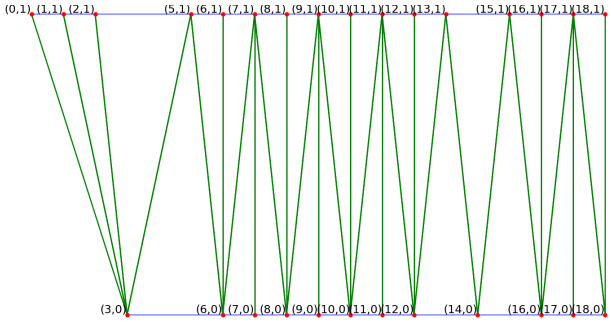

Figure 2. 2D linking in GPS time space. The coordinates represent the scan order: (3, 0) means the 4th point in scan 0, and (0, 1) means the 1st point in scan 1. Some points are missing due to no echo returns. 2D Delaunay triangulation is used to link successive scans.

Figure 3. LiDAR sensor mesh.

mesh from images, we assume that the images are well oriented. Since ray tracing is used for change detection, we need to store the camera position for each vertex of the mesh. Therefore, similar to the LiDAR mesh, we construct a sensor image mesh. Because images are raster data, linking valid pixels naturally produces a mesh. The same strategy as in Figure 2 is used for image sensor mesh generation.

For the dense matching part, we use LiDAR and images to produce the training dataset as in (Wu et al., 2024), and then use PSMNet (Chang and Chen, 2018) to generate disparity maps. Since the images are well oriented, the disparity maps can be converted into point clouds. To improve the quality of the point cloud, multi-view fusion is adopted: (1) one image is selected as the master image, (2) disparity maps are generated for each image pair, and (3) for each pixel in the master image, multi-view forward intersection is applied. The resulting point cloud is shown in Figure 4.

After that, the same strategy as for LiDAR in Figure 2 is used. The resulting point cloud is meshed using the image 2D array structure by building triangles between adjacent points, which we refer to as an image sensor mesh, as shown in Figure 5. The camera center of each point is used as the optical center in ray tracing. If the image mesh is too large, it can be decimated to accelerate further computations. In CGAL, edge collapse (Fabri, 2025) can be used for mesh decimation.

3.3 3D change detection and updating

After generating the sensor meshes from both LiDAR and images, we use ray tracing to detect per-triangle changes (Wu et al., 2023), allowing them to be classified into three classes: consistent, changed (inconsistent areas), or single, as shown in Figure 6. The consistent areas correspond to triangles that are sufficiently close in both meshes; the inconsistent areas correspond to triangles that are intersected by the other mesh during the ray tracing step; and single areas correspond to regions that are covered by only one mesh.

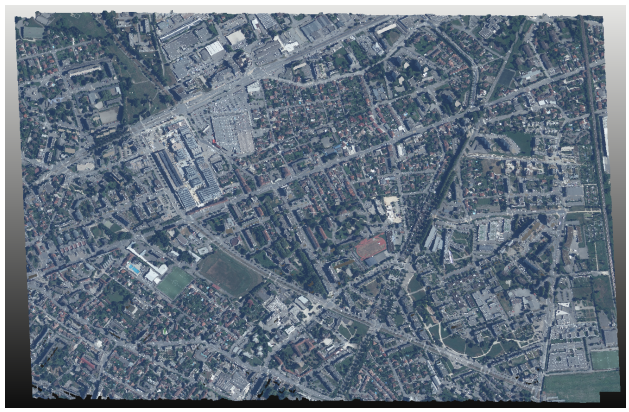

Figure 4. Dense matching point cloud after multi-view fusion.

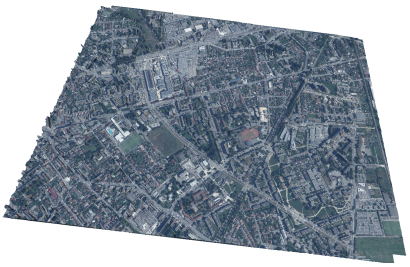

(a) Image sensor mesh

(b) Detail of the sensor mesh

Figure 5. Image sensor mesh shown in MeshLab. The colors represent vertex-based coloring using the master image.

In our case, we only compare two meshes acquired at two different dates, which is simpler than the more general case (Wu et al., 2023). For remote sensing applications, the 3D model often degenerates into a 2.5D representation. In Figure 6(c), even though the image mesh is more recent, the inconsistent areas ③ are not single areas but truly changed regions. Since we know that a new building has been constructed, the ground points in these regions are no longer meaningful and should therefore be removed. For the single areas ⑤, this situation does not occur in our experiments because the LiDAR coverage always includes the image coverage.

The CGAL AABB Tree (Alliez et al., 2025) is used for ray

This contribution has been peer-reviewed. The double-blind peer-review was conducted on the basis of the full paper.
https://doi.org/10.5194/isprs-annals-XI-2-2026-385-2026

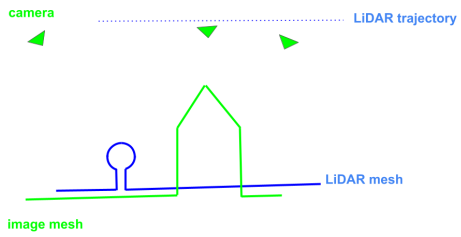

(a) Mesh show in 2D

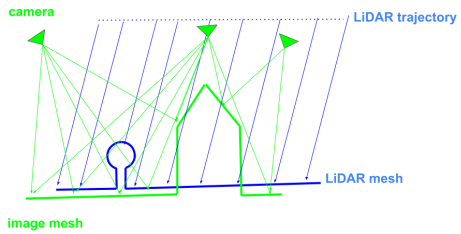

(b) Ray tracing from optical center

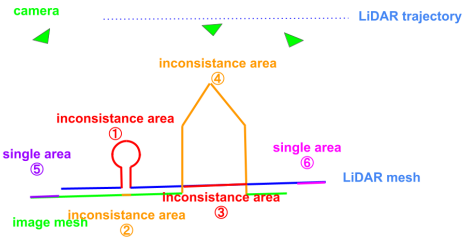

(c) Result after ray tracing

Figure 6. Change detection in 2D. The inconsistent areas ① and ③ need to be removed, inconsistent areas ② and ④ need to be added, single area ⑥is kept, and single area ⑤ is also retained if there is no LiDAR.

tracing in our experiments. After change detection, a simple fusion strategy is applied to update the point cloud: points in the inconsistent areas ① and ③ in Figure 6(c) are removed, while points in the inconsistent areas ② and ④ are fused into the LiDAR point cloud.

4. Experiments and analysis

4.1 Dataset

The LiDAR data used in our experiments come from the French mapping agency (IGN) LiDARHD project, and the aerial images are also collected by IGN. The density of the point cloud is about 10 points/m^2, and the image resolution is 20 cm. The images and LiDAR are well aligned using ground control points, meaning that the image-derived and LiDAR point clouds are well registered.

Two datasets are used, located in the French cities of Grenoble (Isère) and Lyon (Rhône). The coverage area is shown in Figure 7. For the Grenoble dataset, the LiDAR was collected in 2021 and the aerial images in 2024. For the Lyon dataset, the LiDAR was collected in 2021 and the images in 2023.

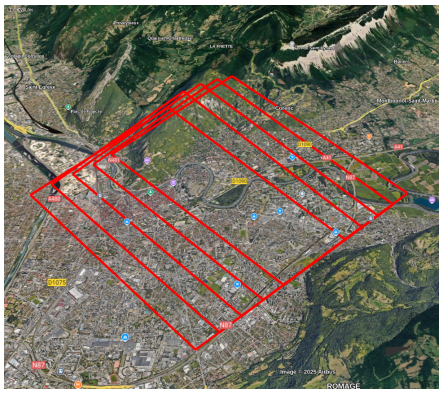

(a) Grenoble dataset

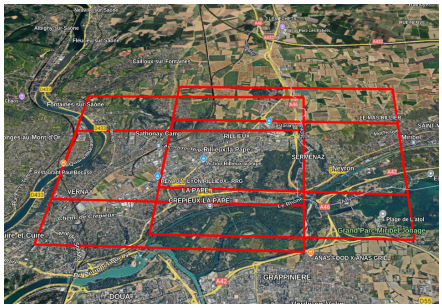

(b) Lyon dataset

Figure 7. Dataset used in the experiment, shown in Google Earth. Red rectangles indicate the image coverage.

4.2 Noise label in training

The quality of the 3D model influences change detection. Considering both accuracy and efficiency, the deep learning–based stereo method PSMNet (Chang and Chen, 2018) is used to produce disparity maps in the experiments. Because deep learning methods rely heavily on training data, their performance decreases when trained on one city and tested on another.

To maximize the quality of the image-derived point cloud, we refine the model using both images and LiDAR to produce the training dataset (Wu et al., 2024). However, due to inconsistencies between the image and LiDAR data, noisy labels appear in the training dataset. The dataset is small, and all available samples are used for training; therefore, overfitting may affect the resulting disparity maps. As a result, changed areas may not be correctly matched, as shown in Figure 8. In the red rectangle in Figure 8(b), there are new buildings, but in the LiDAR point cloud, no buildings are present, as shown in Figure 8(a). The red rectangle in Figure 8(c) indicates a region where the model fails.

Following (Wu et al., 2024), GPU-based Semi-Global Matching (SGM) (Hernandez-Juarez et al., 2016) is used to filter noisy labels. After SGM matching, we compare the disparity map results with the LiDAR-generated disparity map. A 1-pixel error threshold is applied to remove pairs with large discrepancies. Once noisy labels are removed, the model is retrained using the cleaned samples. After that, the performance is improved, as shown in the red rectangle in Figure 8(d).

4.3 Result and analysis

In the experiments, we analyze two types of changes that mainly occur in urban areas: new building construction and

This contribution has been peer-reviewed. The double-blind peer-review was conducted on the basis of the full paper.
https://doi.org/10.5194/isprs-annals-XI-2-2026-385-2026 | © Author(s) 2026. CC BY 4.0 License.

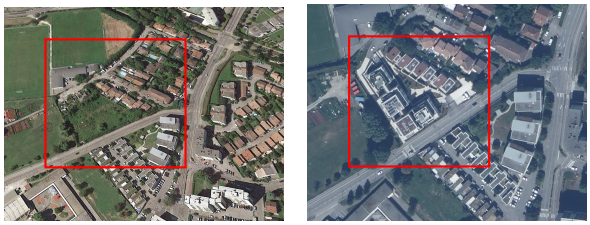

(a) Image 2020 from GoogleEarth (b) Image in 2024

(c) Noise label model result (d) Clean model result

Figure 8. Inconsistencies between the image and LiDAR data (highlighted in the red rectangle) introduce noisy labels in the training dataset, which degrade model performance. These labels must be removed before training.

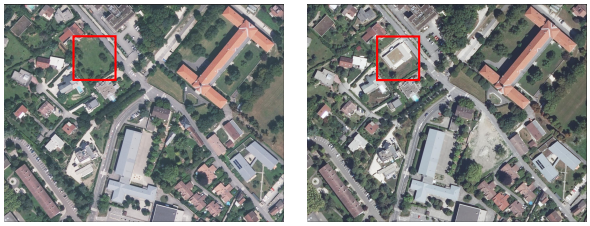

(a) Image in 2021 (b) Image in 2024

Figure 9. New building construction in the Grenoble dataset. The red rectangle shows a new building appearing in 2024.

building demolition.

4.3.1 Building construction In the Grenoble dataset, an example of new building construction is shown in Figure 9. This corresponds to the situation in Figure 6(c), involving inconsistent areas ③ and inconsistent areas ④. This means that ray tracing uses rays from the old mesh (LiDAR mesh), and these rays intersect with the new mesh (image mesh). Unlike (Wu et al., 2023), inconsistent areas are treated as changed regions rather than single parts.

To evaluate the ray tracing results, we color the triangles and visualize them in MeshLab, as shown in Figure 10. The inconsistent areas ③ are marked in red, and the inconsistent areas ④ are marked in orange.

The changed regions are well detected, but due to inaccuracies in the image mesh, some false alarms occur. Small regions are removed based on size thresholds, as shown in Figure 11. As the LiDAR point cloud is more accurate, only the changed parts from the image point cloud are fused into the final point cloud. Afterward, the detected change regions from the image point cloud are integrated into the LiDAR point cloud to obtain the final result, as shown in Figure 12.

4.3.2 Building demolition In the Lyon dataset, an example of building demolition is shown in Figure 13. This corresponds

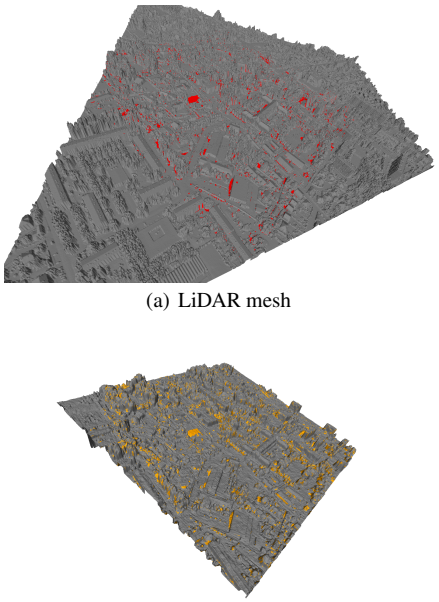

(a) LiDAR mesh

(b) Image mesh

Figure 10. Ray tracing results. Red indicates inconsistent areas ③, and orange indicates inconsistent areas ④. Some false alarms are present.

to Figure 6(c), involving inconsistent areas ① and inconsistent areas ②. Here, ray tracing uses rays from the new mesh (image mesh), and these rays intersect the old mesh (LiDAR mesh), which follows the occupancy theory of ray-based methods.

Similarly, the ray tracing results are shown in Figure 14. The inconsistent areas ① appear in red, and the inconsistent areas ② appear in orange. The changed areas are correctly detected, but inaccuracies in the image mesh again lead to some false alarms. Small regions are removed based on size, as shown in Figure 15, and the remaining change regions are fused into the LiDAR point cloud to obtain the final result, as shown in Figure 16. As the LiDAR point cloud is more accurate, only the changed parts from the image point cloud are fused into the final point cloud.

In the experiment, as shown in Figure 15(b), some false alarms remain in the final result because the building walls are not consistent between the image and LiDAR data.

5. Conclusion

We propose a workflow to update LiDAR point clouds using images, which improves the temporal quality of digital twins. We consider both 3D-based change detection for point clouds and the quality of point clouds during fusion. Because point cloud–based reconstruction remains a challenging task, we propose using sensor meshes derived from LiDAR and images, which are efficient and preserve the optical centers. However, ray tracing in CGAL becomes time-consuming for large meshes, and efficiently handling large areas remains an open issue. The quality of dense matching results influences ray-tracing-based change detection. Failures often occur in occluded areas and vegetated regions, leading to numerous false alarms. Trees are important objects in digital twins, but noise in the resulting point clouds (from both image and LiDAR data) makes tree change detection difficult. In the experiments, only

This contribution has been peer-reviewed. The double-blind peer-review was conducted on the basis of the full paper.
https://doi.org/10.5194/isprs-annals-XI-2-2026-385-2026 | © Author(s) 2026. CC BY 4.0 License.

(a) LiDAR mesh

(b) Image mesh

Figure 11. After removing small areas, most false alarms are eliminated. Red indicates inconsistent areas ③, and orange indicates inconsistent areas ④.

urban areas were studied; updating rural areas remains challenging.

In future work, full mesh-based approaches are also of interest and could provide a direct solution for digital twin reconstruction, although mesh quality will influence the fusion step. On the other hand, ground truth for change detection is not manually annotated in this work, so evaluating the quality of the updates is also an important direction for future research. Semantic information could further enhance change detection by reducing false alarms and preserving true detections in tree-covered areas. Other data sources, such as UAV images, are widely accessible. They offer high temporal resolution, and their use in sustainable change detection is also worth investigating.

6. Acknowledgments

We express our gratitude to Edmond Saint-Denis for providing the dataset. Additionally, we thank CNES (French space agency) for granting access to the HAL (High Performance Computing) GPU cluster.

References

Aijazi, A., Checchin, P., Trassoudaine, L., 2013a. Detecting and updating changes in lidar point clouds for automatic 3d urban cartography. *ISPRS annals of the photogrammetry, remote sensing and spatial information sciences*, 2, 7–12.

Aijazi, A. K., Checchin, P., Trassoudaine, L., 2013b. Automatic removal of imperfections and change detection for accurate 3D urban cartography by classification and incremental updating. *Remote Sensing*, 5(8), 3701–3728.

Alliez, P., Tayeb, S., Wormser, C., 2025. 2D and 3D fast intersection and distance computation. *CGAL User and Reference Manual*, 6.1 edn, CGAL Editorial Board.

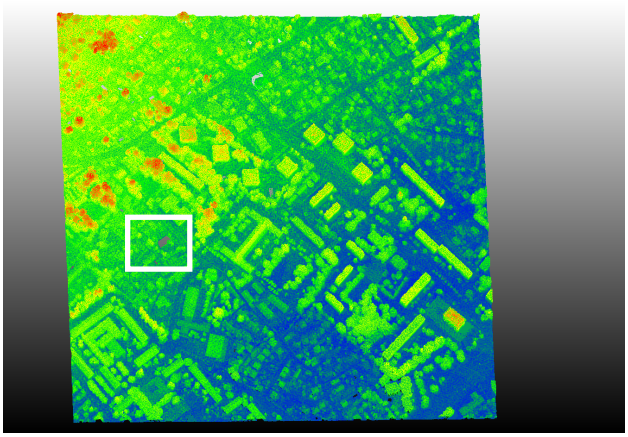

(a) Remaining LiDAR point cloud

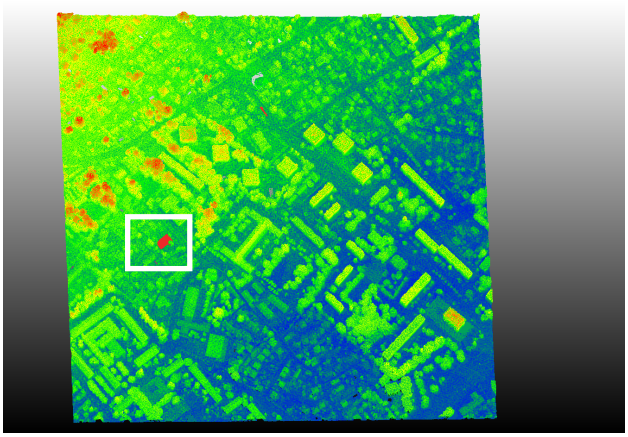

(b) Fused LiDAR and image point cloud

Figure 12. Final result for Grenoble: after removing the detected changes and fusing the image-derived points into the LiDAR point cloud. The white rectangle indicates the change area. Red points are from image-based dense matching.

Bai, T., Wang, L., Yin, D., Sun, K., Chen, Y., Li, W., Li, D., 2023. Deep learning for change detection in remote sensing: a review. *Geo-spatial Information Science*, 26(3), 262–288.

Boussaha, M., Vallet, B., Rives, P., 2018. Large scale textured mesh reconstruction from mobile mapping images and lidar scans. *ISPRS Annals of the Photogrammetry, Remote Sensing and Spatial Information Sciences*, 4, 49–56.

Chang, J.-R., Chen, Y.-S., 2018. Pyramid stereo matching network. *Proceedings of the IEEE conference on computer vision and pattern recognition*, 5410–5418.

Du, S., Zhang, Y., Qin, R., Yang, Z., Zou, Z., Tang, Y., Fan, C., 2016. Building change detection using old aerial images and new LiDAR data. *Remote Sensing*, 8(12), 1030.

Fabri, A., 2025. 2D polyline simplification. *CGAL User and Reference Manual*, 6.1 edn, CGAL Editorial Board.

Hernandez-Juarez, D., Chacón, A., Espinosa, A., Vázquez, D., Moure, J. C., López, A. M., 2016. Embedded real-time stereo estimation via semi-global matching on the GPU. *Procedia Computer Science*, 80, 143–153.

Kazhdan, M., Bolitho, M., Hoppe, H., 2006. Poisson surface

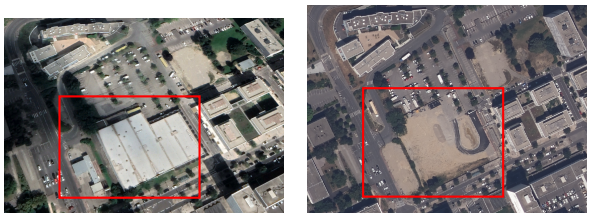

(a) Image 2021 from GoogleEarth (b) Image in 2023

Figure 13. Building demolition in the Lyon dataset. The red rectangle highlights areas where two buildings were removed by 2023.

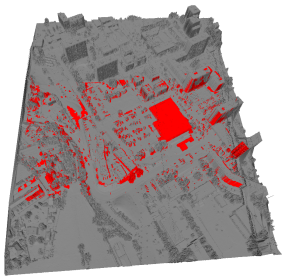

(a) LiDAR mesh

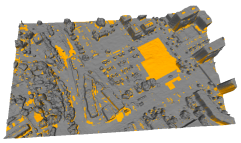

(b) Image mesh

Figure 14. Ray tracing results. Red indicates inconsistent areas ①, and orange indicates inconsistent areas ②. Some false alarms are present.

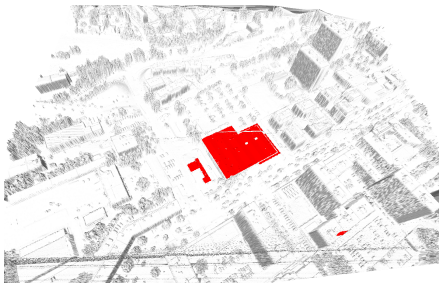

(a) LiDAR mesh

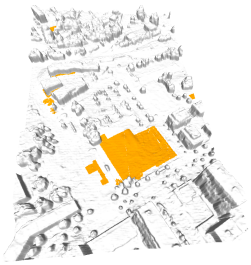

(b) Image mesh

Figure 15. After removing small areas, most false alarms are eliminated. Red indicates inconsistent areas ①, and orange indicates inconsistent areas ②.

reconstruction. *Proceedings of the fourth Eurographics symposium on Geometry processing*, 7number 4.

Labatut, P., Pons, J.-P., Keriven, R., 2009. Robust and efficient surface reconstruction from range data. *Computer graphics forum*, 28number 8, Wiley Online Library, 2275–2290.

Laga, H., Jospin, L. V., Boussaid, F., Bennamoun, M., 2020. A survey on deep learning techniques for stereo-based depth estimation. *IEEE transactions on pattern analysis and machine intelligence*, 44(4), 1738–1764.

Pang, C., Wu, J., Ding, J., Song, C., Xia, G.-S., 2023. Detecting building changes with off-nadir aerial images. *Science China Information Sciences*, 66(4), 140306.

Qin, R., Gruen, A., 2014. 3D change detection at street level using mobile laser scanning point clouds and terrestrial images. *ISPRS Journal of Photogrammetry and Remote Sensing*, 90, 23–35.

Remondino, F., Spera, M. G., Nocerino, E., Menna, F., Nex, F., 2014. State of the art in high density image matching. *The photogrammetric record*, 29(146), 144–166.

Stilla, U., Xu, Y., 2023. Change detection of urban objects using 3D point clouds: A review. *ISPRS Journal of Photogrammetry and Remote Sensing*, 197, 228–255.

Sulzer, R., Marlet, R., Vallet, B., Landrieu, L., 2024. A survey and benchmark of automatic surface reconstruction from point clouds. *IEEE Transactions on Pattern Analysis and Machine Intelligence*.

Swart, L., 2010. How the Up-to-date Height Model of the Netherlands (AHN) became a massive point data cloud. *NCG KNAW*, 17, 17–32.

Vu, H.-H., Labatut, P., Pons, J.-P., Keriven, R., 2011. High accuracy and visibility-consistent dense multiview stereo. *IEEE transactions on pattern analysis and machine intelligence*, 34(5), 889–901.

Waechter, M., Moehrle, N., Goesele, M., 2014. Let there be color! large-scale texturing of 3d reconstructions. *European conference on computer vision*, Springer, 836–850.

Wang, R., 2013. 3D building modeling using images and LiDAR: A review. *International Journal of Image and Data Fusion*, 4(4), 273–292.

Wang, X., Wang, C., Liu, B., Zhou, X., Zhang, L., Zheng, J., Bai, X., 2021. Multi-view stereo in the deep learning era: A comprehensive review. *Displays*, 70, 102102.

Wen, D., Huang, X., Bovolo, F., Li, J., Ke, X., Zhang, A., Benediktsson, J. A., 2021. Change detection from very-high-spatial-resolution optical remote sensing images: Methods, applications, and future directions. *IEEE Geoscience and Remote Sensing Magazine*, 9(4), 68–101.

Wu, T., Hu, X., Zhang, Y., Zhang, L., Tao, P., Lu, L., 2016. Automatic cloud detection for high resolution satellite stereo images and its application in terrain extraction. *ISPRS Journal of Photogrammetry and Remote Sensing*, 121, 143–156.

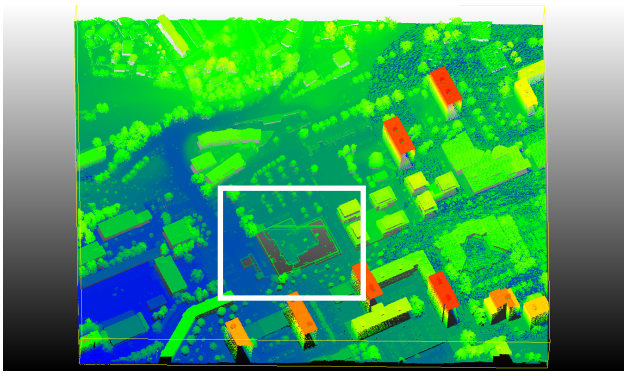

(a) Remaining LiDAR point cloud

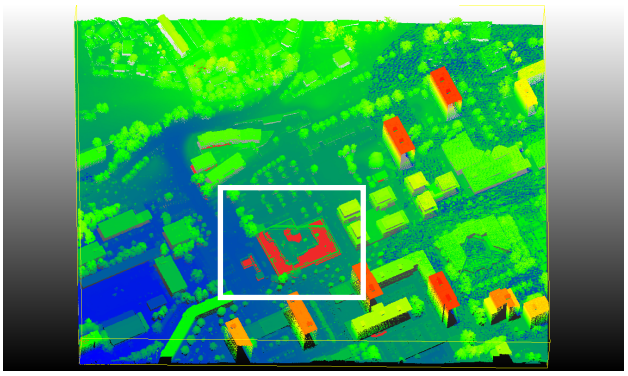

(b) Fused LiDAR and image point cloud

Figure 16. Final result for Lyon: after removing the detected changes and fusing the image-derived points into the LiDAR point cloud. The white rectangle indicates the change area. Red points are from image-based dense matching.

Wu, T., Vallet, B., Demonceaux, C., 2023. Mobile Mapping Mesh Change Detection and Update. *arXiv preprint arXiv:2303.07182*.

Wu, T., Vallet, B., Pierrot-Deseilligny, M., Rupnik, E., 2024. An evaluation of Deep Learning based stereo dense matching dataset shift from aerial images and a large scale stereo dataset. *International Journal of Applied Earth Observation and Geoinformation*, 128, 103715.

Xiao, W., Cao, H., Tang, M., Zhang, Z., Chen, N., 2023. 3D urban object change detection from aerial and terrestrial point clouds: A review. *International Journal of Applied Earth Observation and Geoinformation*, 118, 103258.

Xiao, W., Vallet, B., Brédif, M., Paparoditis, N., 2015. Street environment change detection from mobile laser scanning point clouds. *ISPRS Journal of Photogrammetry and Remote Sensing*, 107, 38–49.

Zhang, Y., Xia, B., Taylor, S., 2024. High-resolution 3-D geometry updating of digital functional models using point cloud processing and surface cut. *Computer-Aided Civil and Infrastructure Engineering*, 39(1), 3–19.

Zhou, K., Lindenbergh, R., Gorte, B., Zlatanova, S., 2020. LiDAR-guided dense matching for detecting changes and updating of buildings in Airborne LiDAR data. *ISPRS Journal of Photogrammetry and Remote Sensing*, 162, 200–213.